

Propagation Delay Comparison between Single-Walled CNT Bundle and Multi-Layered GNR for Global VLSI Interconnects

Pankaj Kumar Das

Abstract—In the era of nanotechnology, Carbon Nanotube (CNT) and Graphene Nanoribbon (GNR) have potentially gained reputation as emerging material for VLSI interconnects. This paper primarily introduces an equivalent single conductor (ESC) model of single-walled carbon nanotube (SWCNT) bundle and multilayer graphene nanoribbons (MLGNRs). The ESC model is used to compare the propagation delay of SWCNT bundle and MLGNRs for different interconnect lengths. It has been observed that on an average, MLGNRs reduces the propagation delay by 96.62% compared to SWCNT bundle structure at global VLSI interconnect lengths.

Index Terms— Carbon nanotube (CNT), single-walled CNT (SWCNT), Graphene nanoribbon (GNR), multi-layer GNR (MLGNR), equivalent single conductor (ESC), interconnect, propagation delay.

I. INTRODUCTION

IN current nanoscale regime, carbon nanotubes (CNTs) and graphene nanoribbons (GNRs) have emerged as a novel material for VLSI interconnects [1]. CNTs and GNRs have considered as possible replacement of Cu because of their outstanding performance as high speed global VLSI interconnects [1-5]. The outstanding electrical as well as mechanical properties such as higher current density [4], long ballistic transport length [4], higher tensile strength [3], makes them a perfect interconnect material at current nanoscale regime.

Graphene, a flat two dimensional mono atomic layer sheet of carbon allotrope, has emerged as an extra ordinary material of the 21st century for interconnect design, and has potentially gained worldwide attention due to am bipolar carrier conduction [6]. Graphene has defect density of $\sim 1 \times 10^{10}/\text{cm}^2$ [7] and higher carrier mobility of more than $10^6 \text{cm}^2/\text{V}\cdot\text{sec}$. This mobility is practically independent of temperature, thus opening the opportunity of room temperature ballistic transport at the sub-micrometer scale. The electronic states of GNRs mainly depend on the edge structures [6-7]. Zigzag edges provide the edge-localized state with non-bonding molecular orbital's near the Fermi energy. Zigzag GNRs are always metallic while armchairs can be either metallic or semiconducting [6-7]. The, metallic

properties of ac-GNRs governed by the condition of $M=3n-1$ or $3n+2$ whereas $M=3n$ or $3n+1$ satisfies the semiconducting properties in which n can be defined as an integer [7]. However, the zz-GNRs are always shows the metallic behavior independent of M , where M is the number of hexagonal rings across the width. Depending on the number of graphene layers formed by the hexagonal rings of carbon atoms, GNR can be classify as single-layer GNR (SLGNR) and multi-layer GNR (MLGNR). SLGNR is having relatively high electrical conductance. However, MLGNR is preferred in modern interconnect applications because of their relatively low equivalent resistance [7].

The organization of this paper is as follows: Section I introduces the remarkable properties of novel interconnect materials like, CNT and GNR. The bundle geometry and generalized ESC model of SWCNT and MLGNR interconnects are presented in section II. Simulation setup using a driver-interconnect-load (DIL) system is introduces in section III. Section IV compares the propagation delay of SWCNT bundle and MLGNR. Finally, section V concludes the paper.

II. GEOMETRY AND EQUIVALENT RLC MODEL FOR BUNDLED SWCNT AND MLGNR INTERCONNECTS

A. Geometry of Bundled SWCNT

The Geometry of SWCNT bundle above the ground plane is shown in fig. 1 that consists of number of SWCNTs having same diameter placed inside the bundle. The spacing between SWCNTs (δ) in bundle is determined by vander waals forces between the atoms in adjacent nanotubes. The probability of semiconducting to metallic nanotubes inside the bundle $\beta = 1/3$. Total number SWCNTs in bundle is approximated as [8]

$$N_{SWCNT} = \left[N_x N_y - \text{Integer} \left(\frac{N_y}{2} \right) \right] \quad (1)$$

where N_x and N_y are the number of SWCNTs in bundle facing to the surface at horizontal and vertical directions, respectively. The center-to-center distance between adjacent SWCNTs in bundle can be expressed as [9]

$$d_b = \delta + d \quad (2)$$

Pankaj Kumar Das is serving as Assistant Professor at Sant Longowal Institute of Engineering and Technology, Longowal- 148106, India (Phone: +911672-253331; fax: +911672-253100; e-mail: pankaj.jkd@gmail.com).

where $\delta = 0.34\text{nm}$ is the spacing between SWCNTs in bundle and d is the diameter of individual SWCNT.

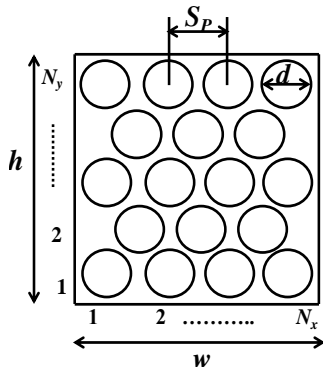


Fig. 1. Cross-section of a SWCNT bundle interconnects

B. Geometry of MLGNR

The geometry of MLGNR over a dielectric plane is shown in Fig. 2 that consists of number of single GNR layers of lengths l . The thickness t and width W of MLGNR is determined by the technology node. The spacing between GNR layers $\delta = 0.34\text{nm}$ or inter layer spacing is determined by vander waals forces between the atoms in adjacent graphene layers. As per the technology node and considering the thickness and width of MLGNR the total number of graphene layers in MLGNR can be approximated as [10]

$$N_{\text{layer}} = 1 + \text{Integer}(t/\delta) \quad (3)$$

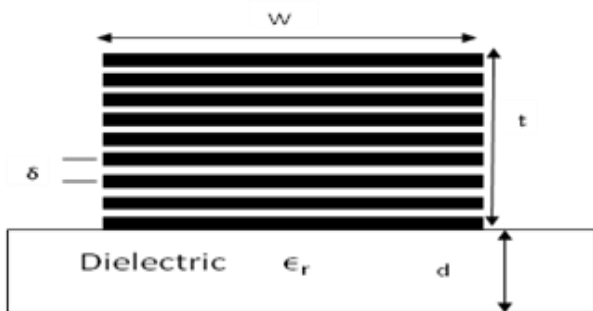


Figure 2. Geometry of MLGNR [11]

C. RLC model for bundled SWCNT and MLGNR

The detailed description of RLC model of bundled SWCNT and MLGNR interconnect is presented based on modeling approach for MWCNT bundle [8]. The equivalent RLC model consists of metal-nanotube imperfect contact resistance or metal graphene sheet imperfect contact resistance (R_C) with a typical value of $3.2\text{K}\Omega$. Each SWCNT or GNR layer exhibits (1) quantum or intrinsic resistance (2) imperfect metal-nanotube/graphene contact resistance (R_{mc}) (3) scattering resistance R' . The SWCNT/graphene has four conducting channels due to spin degeneracy and sublattice degeneracy. Depending on the total number of conducting channel of bundle, the total bundle resistance appears as [8]

$$R_{ESC} = R_{C,ESC} + R'_{ESC} \cdot L \quad (4)$$

$$R_{C,ESC} = \left[\sum_{i=1}^n \left(\frac{R_q}{2N_i} + R_{mc,i} \right)^{-1} \right]^{-1}, \quad R_q = h / 2e^2 \quad (5)$$

$$R'_{ESC} = \left(\sum_{i=1}^n \frac{2N_i}{R_q} \lambda_{mfp,i} \right)^{-1} \quad (6)$$

Where, N_i is the conducting channel of i^{th} SWCNT/graphene and n is the number of SWCNT/grapheme layer.

The equivalent circuit also consists of kinetic inductance (L_K) which basically arises due to kinetic energy of electrons and can be expressed for SWCNT bundle/MLGNR as [8, 10, and 12]

$$L_{K,ESC} = \frac{L_k}{2N_{\text{total}}} \quad (7)$$

Where, $L_K = \frac{h}{2e^2 v_F}$ and N_{total} is the total number of conducting channel of SWCNT bundle/MLGNR.

The equivalent capacitance of the ESC model includes two types of capacitances: electrostatic capacitance ($C_{E,ESC}$) and quantum capacitance ($C_{Q,ESC}$). The electrostatic capacitances and quantum capacitances can be expressed as [8, 10 and 12]

$$C_{E,ESC} = N_x 2\pi\epsilon_0\epsilon_r / \cosh^{-1} \left[\left(\frac{D_n + 2h_t}{D_n} \right) \right] \quad (8)$$

$$C'_{Q,ESC} \approx 2N_{\text{total}} C_q \quad (9)$$

Where, $C_q = 2e^2/hv_f$, e = electronic charge, v_f = fermi velocity of graphene sheet.

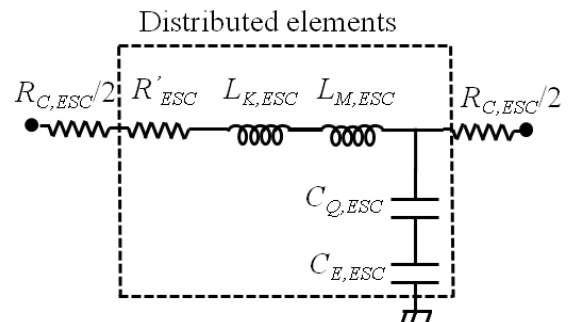


Fig. 3. Equivalent RLC model [8]

III. SIMULATION SETUP

This paper, primarily analyzes the propagation delay for bundled SWCNT and MLGNR at different interconnects lengths ranging from $400\mu\text{m}$ to $2000\mu\text{m}$ and compared. The interconnect line is replaced by the equivalent RLC model of bundled SWCNT and MLGNR structure. Simulation setup uses CMOS inverter at 32nm technology node. The interconnect line is terminated with a load capacitance $C_L = 10\text{aF}$.

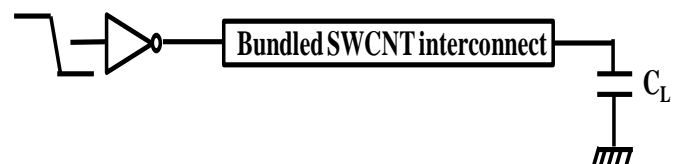


Fig. 3. Driver- interconnects load (DIL) system.

IV. RESULT AND DISCUSSIONS

HSPICE simulations are performed for bundled SWCNT and MLGNR structures to address the propagation delay at different interconnects lengths. The propagation delay increases with interconnect lengths but the propagation delay of MLGNR is reduces in comparisons with SWCNT bundle. The reason behind is that the propagation delay mainly depends on interconnects parasitic such as capacitance, inductance and resistance. The increasing number of conducting channel in MLGNR reduces interconnects parasitic inductances and resistances results decreases the propagation delay.

Finally, the propagation delay for SWCNT bundle and MLGNR is presented and summarized in Table 1. It has been observed that propagation delay significantly reduces for MLGNR compared to SWCNT bundle.

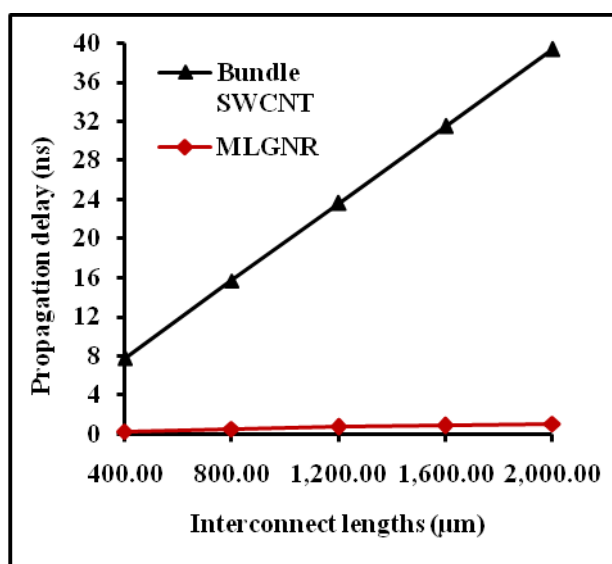


Figure 1. Propagation delay comparison between SWCNT bundle and MLGNR.

TABLE I.

PROPAGATION DELAY FOR SWCNT BUNDLE AND MLGNR AT DIFFERENT GLOBAL INTERCONNECT LENGTHS

Interconnect lengths (µm)	Propagation delay (in ns) for SWCNT bundle and MLGNR	
	SWCNT Bundle	MLGNR
400	7.751	0.271
800	15.702	0.497
1200	23.590	0.684
1600	31.473	0.839
2000	39.371	0.997

V. CONCLUSION

This research paper primarily introduces two structures SWCNT bundle and MLGNR for VLSI interconnects design. Propagation delay has been analyzed and compared between bundled SWCNT and MLGNR at different global VLSI interconnect lengths. It has been observed that propagation delay mainly depends on interconnect parasitic that is mainly depends on total number of conducting

channel of bundle structure. Based on simulation results it has been observed that, on an average the propagation delays are reduced by 96.62% for MLGNR compared to bundle SWCNT.

REFERENCES

- [1] H. Li, C. Xu, N. Srivastava and K. Banerjee, "Carbon Nanomaterials for Next-Generation Interconnects and Passives: Physics, Status and Prospects," *IEEE Trans. Electron Devices*, vol. 56, no. 9, pp. 1799-1821, Sep. 2009
- [2] A. Javey and J. Kong, *Carbon Nanotube Electronics*, Springer, 2000.
- [3] R. Satio, G. Dresselhaus and S. Desselhaus, *Physical Properties of Carbon Nanotubes*. London, U. K.: Imperial College Press, 1998.
- [4] B. Q. Wei, R. Vajtai, and P. M. Ajayan, "Reliability and current carrying capacity of carbon nanotubes," *Appl. Phys. Lett.*, vol. 79, no. 8, pp. 1172-1174, 2001.
- [5] P. G. Collins, M. Hersam, M. Arnold, R. Martel, and P. Avouris, "Current saturation and electrical breakdown in multiwalled carbon nanotubes," *Phys. Rev. Lett.*, vol. 86, no. 14, pp. 3128-3131, 2001.
- [6] C. Xu, H. Li, and K. Banerjee, "Graphene Nano-Ribbon (GNR) Interconnects: A Genuine Contender or a Delusive Dream?," in Proc. *IEEE IEDM*, pp.1-4, 2008.
- [7] A. Naeemi and J. D. Meindl, "Conductance modeling for grapheme nanoribbon (GNR) interconnects," *IEEE Electron Device Lett.*, vol. 28, no. 5, pp. 428-431, May 2007.
- [8] Majumder MK, Das PK, Kaushik BK, "Delay and crosstalk reliability issues in mixed MWCNT bundle interconnects" *Microelectronics Reliability, Elsevier*, vol. 54, pp. 2570-2577, 2014.
- [9] A. Srivastava, Y. Xu, and A. K. Sharma, "Carbon nanotubes for next generation very large scale integration interconnects," *Journal of Nanophotonics*, vol. 4, no. 041690, pp. 1-26, May 2010.
- [10] J. -P. Cui, W. -S. Zhao, and W. -Y. Yin "Signal Transmission Analysis of Multilayer Graphene Nano-Ribbon (MLGNR) Interconnects," *IEEE Trans. Electromagnetic Compatibility*, vol. 54, no. 1, pp.126-132, Feb. 2012.
- [11] Reddy Narasimha, Majumder MK, Kaushik BK, B. Anand and Das PK, "Optimized Delay and Power Performances in Multi-layer Graphene Nanoribbon Interconnects" in Proc. *IEEE Asia Pacific Conference on Postgraduate Research in Microelectronics & Electronics*, PP-122-125, 2012.
- [12] P. J. Burke, "Luttinger Liquid Theory as a Model of the Gigahertz Electrical Properties of Carbon Nanotubes," *IEEE Trans. Nanotechnology*, vol. 1, no. 3, Sep. 2002.